Correlating Cell Distance with Sympathetic Alignment

Thesis by
Rohit Ravichandran

In Partial Fulfillment of the Requirements for the
Degree of
Master of Chemical Engineering

Advisor: Victor Barocas

University of Minnesota, Twin Cities
Minneapolis, Minnesota

2025

ACKNOWLEDGEMENTS

I would like to express my gratitude to Adam Ley for his guidance and encouragement throughout this research. Furthermore, thank you to Professor Victor Barocas for providing the opportunity to work in his lab and serving as the lead on my thesis committee. I also thank my other committee members, Professor Kevin Dorfman and Professor Patrick Alford, for their insightful comments and support.

ABSTRACT

Contact guidance is the tendency of cells to reorient themselves with one another and migrate due to anisotropy like aligned fibrins, serving purpose in sustaining healthy tissue as well as promoting cancer progression. To better understand contact guidance, a computational tool is developed to analyze cell migration and elongation in fibrin gels as distance between cells are varied. The results indicated that cells tend not to elongate when closer together and sees more elongation farther apart, while the opposite trend is seen for cell alignment. These results do not fully align with the hypothesis, opening discussion for improvement opportunities with the tool.

TABLE OF CONTENTS

LIST OF TABLES

LIST OF FIGURES

NOMENCLATURE

Extracellular Matrix: non-cellular component of the tissue that plays a crucial role in structural support and cell signaling.

Contact Guidance: phenomenon where cells tend to align themselves in the direction of collagen fibers or other structures.

Durotaxis: the tendency of cells to move in the direction of increasing stiffness gradients.

ODF: Ovine Dermal Fibroblasts (sheep cells). These are used in this study.

CHAPTER 1: INTRODUCTION

1.1 Background

Cancer is one of the most significant global health issues due to its ability to rapidly reproduce and spread throughout the human body. The American Cancer Society estimated 20 million new cases and 9.7 million deaths in 2024.[1] While significant progress has been made in cancer treatment—particularly with established methods like radiation therapy and chemotherapy—there is still considerable room for improvement. Ongoing research aims to enhance the effectiveness of these therapies and develop new approaches to more precisely target and eliminate cancerous cells.

1.2 Extracellular Matrix

The extracellular matrix, ECM, is generally known as the non-cellular component of the tissue that plays a role in structural support. However, the ECM is a crucial mediator in cell adhesion and cell behavior modulation, as in how cells communicate with their surroundings, proliferate, and migrate, signal regulation, and tissue repair.[2] Primary components of the ECM are collagen or elastin, which are examples of protein fibers. The fibers have anisotropic alignment where the tissue has higher tensile strength and stiffness in the direction of the fiber's alignment.

The ECM plays a crucial role in tumor microenvironment growth. During cancer progression, the ECM undergoes significant remodeling, resulting in changes with stiffness, composition, and structural orientation that will ultimately aid in tumor initiation, growth, and progression.[2] As outlined in figure 1 proliferation of epithelial neoplastic cells causes the membrane to break down, and the increased stiffness of the ECM triggers signaling pathways, and the aligned fibers aid with cancer cell migration.

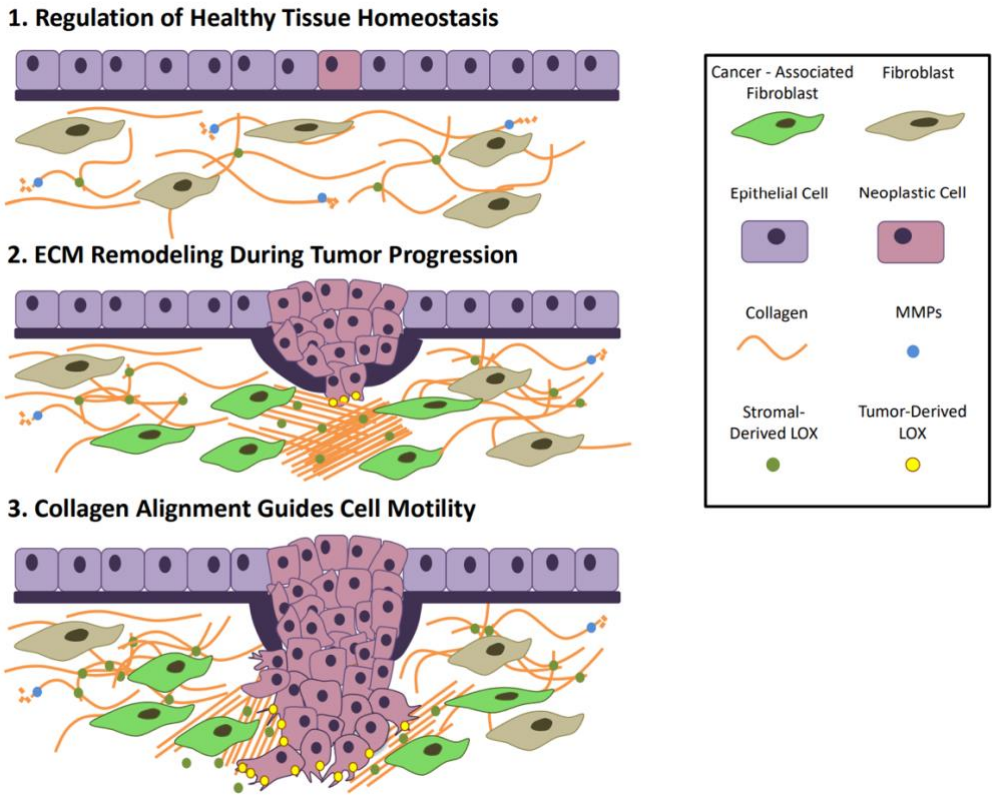

Figure 1: ECM remodeling during cancer initiation and progression. (1) Proliferation of epithelial neoplastic cells. (2) The basement membrane expands due to the proliferation of the cells. (3) Neoplastic cells break through the membrane and go along the aligned. Reproduced from Ref. 2.

With this, understanding how cells interact with the ECM cues in healthy and diseased tissue are crucial and may provide a promising pathway to cancer therapeutics.

1.3 Contact Guidance

Contact guidance is a phenomenon where cells tend to align themselves in the direction of collagen fibers or other structures,[3] showcased in figure 2. Contact guidance provides insight on how cells promote preferential alignment and is different from durotaxis as contact guidance can result in bidirectional anisotropy.

Studies have been conducted on 1D and 2D systems for contact guidance. In 1D, cell migration experiments in nanofiber microenvironments revealed increased alignment along the fibers.[4] In 2D, studies observed that the aligned structures increase cell migration, alignment, and speed.[5]

These results show similarities to durotatic cues. 3D systems have been explored as well, which further support the findings of 2D systems.[6-7]

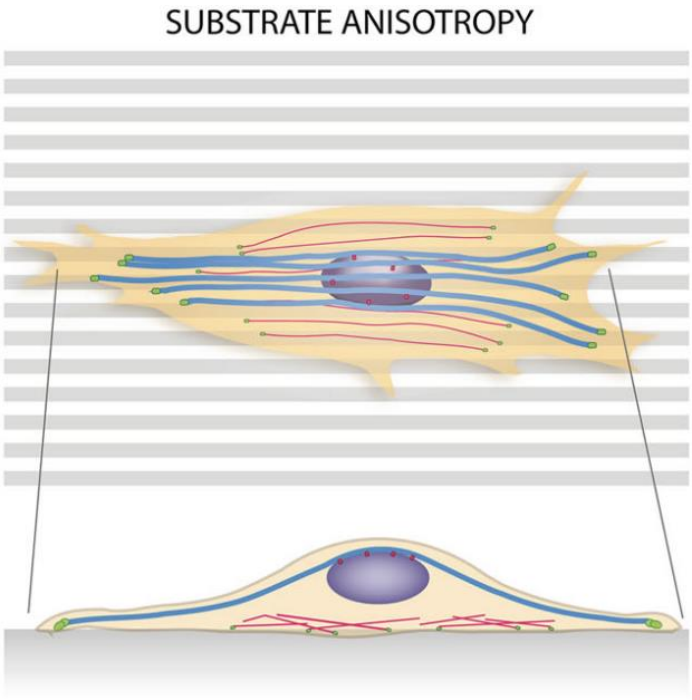

Figure 2: Visual representation of cellular response to substrate anisotropy. Reproduced from Ref. 7.

Current models and simulations can emulate cell migration from contact guidance. In all three systems, some variations of random walk or anisotropic random walk models have been utilized.[8-10] Furthermore, to get insight on the guidance field, studies have been conducted on cell movement by using mechanically constrained fibrin gels by fibroblasts. But the field cannot be defined or controlled due to the complex system of interdependent and simultaneous signaling to the cells.[3] There is limited research in quantifying contact guidance, particularly for analyzing pairs of neighboring cells and seeing how contact guidance varies when the distance between cells is changed.

Another reason for the lack of progress in this is due to the difficulty of changing just one of the anisotropies while keeping the others unchanged. Understanding anisotropies of contact

guidance poses significant challenges compared to other cell migration mechanisms as the other mechanisms have clear signals.

1.4 Durotaxis

Durotaxis is a concept where cells move in the direction of increasing stiffness gradients. The foundation to this was Dunn's hypothesis, in which he theorized that cells alter their behaviors and alignment by sensing chemical, mechanical, and steric anisotropies, shown in figure 3.

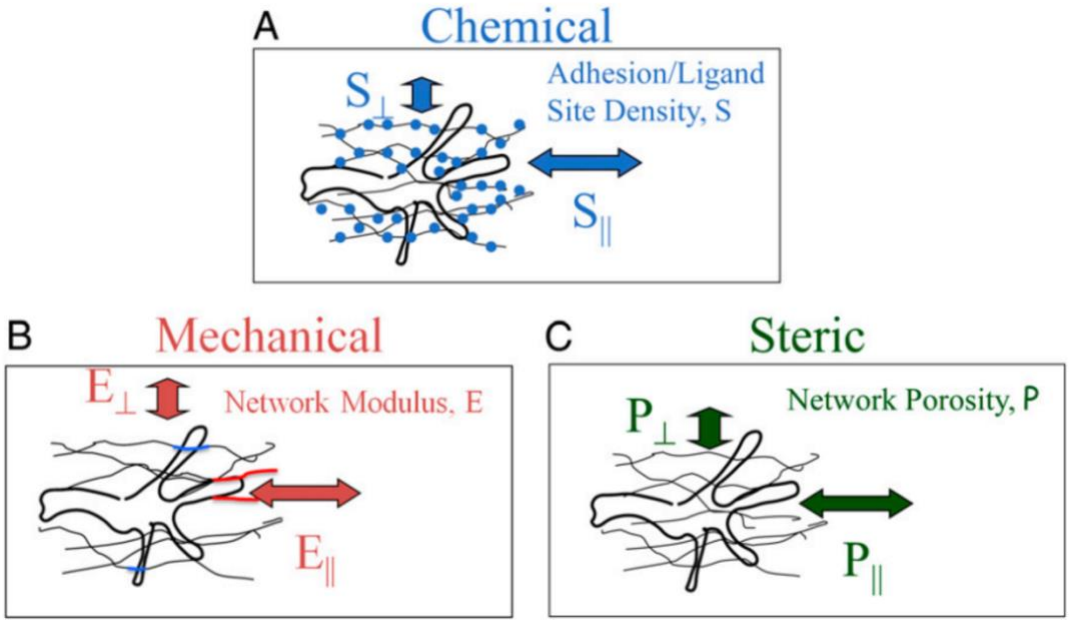

Figure 3: Visualization of Dunn's hypotheses for signal-inducing contact guidance of cells in aligned fibrils. (A) Chemical adhesion anisotropy process, in which the blue dots represent cell-binding sites. (B) Stiffness anisotropy. (C) Steric anisotropy. Reproduced from Ref. 3.

Current work on the effects of durotaxis have been explored in 2D and 3D using the photo crosslinking chemistry of continuous and step gradients.[11-13] In 2D, studies showcased that cells move to a direction of optimal stiffness. In addition, studies also showed evidence of negative durotaxis, in which cells move in regions of lower stiffness. So, in 2D, it is found that there may exist an optimal stiffness. Additional opportunities are present in understanding how cell

reorientation and migration are influenced by durotaxis. Durotaxis can be extended to cancer cell mechanics as well, as these cues play a critical role in cancer progression. But there are limited studies on the effects of durotactic cues on cancer cells as well.

1.5 Project Scope

This project presents a new approach to addressing the discussed knowledge gaps through the development of a foundational computational tool that can characterize cell elongation, alignment, and orientation. More importantly, this study aims to seek understanding of the cell-ECM-cell signaling mechanism.

Ovine dermal fibroblasts (ODF), or sheep cells, were placed in the fibrin hydrogels and are imaged via microscopy. Gels are produced in triplicate and imaged at several points throughout the gel. In 2D, the tool quantified the cells' "roundness" or circularity factor and analyze how cell elongation varies as the distance between the paired cells changes. Based on the observational results of contact guidance, the expectation is that cells will align and elongate more when closer together. In terms of the tool, it means the average circularity and the angle formed between cells should be smaller.

CHAPTER 2: METHODS

2.1 Experimental Methods

2.1.1 Fibrin Gel Casting

To begin the procedure, Corning grease was used to attach the mold to the glass well plate. The mold was then sterilized by treating it with alcohol for 30 minutes and UV exposure inside a biosafety hood. Then, the mold was washed three times using sterile Dulbecco's Phosphate Buffered Saline (DPBS) to remove any residual alcohol. A suspension of 6 mg/mL fibrinogen, from bovine plasma, was made with the DPBS. The suspension was sterilized using a Steriflip filter with a 200 μm pore size. Separately, the following two suspensions were made: one with an activated thrombin solution at 1.2 U/mL and the other with the ODF cells at 180,000 cells/mL. The reagents were then placed on ice to prevent premature crosslinking. Then, the fibrinogen, thrombin, and cell suspensions were combined in a 4:1:1 volume ratio. So, the final gel yielded a composition of 4 mg/mL fibrin, 0.2 U/mL thrombin, and 30,000 cells/mL. Using the pipette, the final suspension was thoroughly mixed, and 400 μL of the solution was dispensed into each mold. To allow gel formation, the molds were left for 30 minutes incubated and undisturbed. After gelation, pre-warmed complete media—composed of DMEM/F12 supplemented with 10% fetal bovine serum (FBS) and 1% Penicillin/Streptomycin—were added to each well. Finally, the plates were incubated for 24 hours, allowing the cells to settle and interact within the matrix. In this study, the gel plates were created in triplicate.

2.1.2 Fixation and Staining

After the 24-hour incubation was completed, cell media was aspirated from the well plates. Then, 1 mL of 4% paraformaldehyde (PFA) was added to each well and incubated for 20 minutes, allowing for cell fixation. The PFA is washed out DPBS in triplicate after the fixation. The cells were then permeabilized by adding 0.1% Triton X-100 in DPBS and incubated for 30 minutes. Then, DPBS wash was performed in triplicate to wash out the solution. Next, a 2.5% bovine serum albumin (BSA) solution in DPBS was mixed in with the cells and incubated for 30 minutes to block non-specific binding. Then, the staining solutions were added directly to the cells. Alexa Fluor Phalloidin 594 was the stain to label actin filaments and Hoechst 33342 to stain cell nuclei. The plates were incubated overnight at 4°C to ensure proper staining. The next day, the wells were washed with DPBS in triplicate to remove excess stain.

2.1.3 Fluorescent Imaging and Microscopy

Imaging was performed using fluorescent microscope in a dark room. The scope had a 4x objective lens and a 10x eyepiece, which yielded a total magnification of 40x. For the actin staining, images used a 594 nm excitation and 615 nm emission. For nuclear staining, images used a 405 nm excitation and 450 nm emission. The z-stack images were taken at over a 500 μm depth, starting at 50 μm above the glass surface of the well to avoid imaging the cells adhered to the glass well.

2.2 Computational Method

The key element of this project was the development of a computational tool, via MATLAB, that can analyze the positions, morphology, and give quantitative insight on how cell properties vary with varies with distance. Image stacks derived from the Hoechst 33342 staining

(nuclear) were denoted C00, and image stacks from the Alexa fluor phalloidin 594 staining (actin) were denoted C01. However, the focus of this project was only the C01 image stacks.

2.2.1 Sensitivity Analysis

To better enhance the cellular regions from the background, the image stacks are binarized using Otsu's method,[14] in which the color variance within the cellular structures are minimized while the variance between the cellular structures and the background is maximized, as illustrated in figure 4.

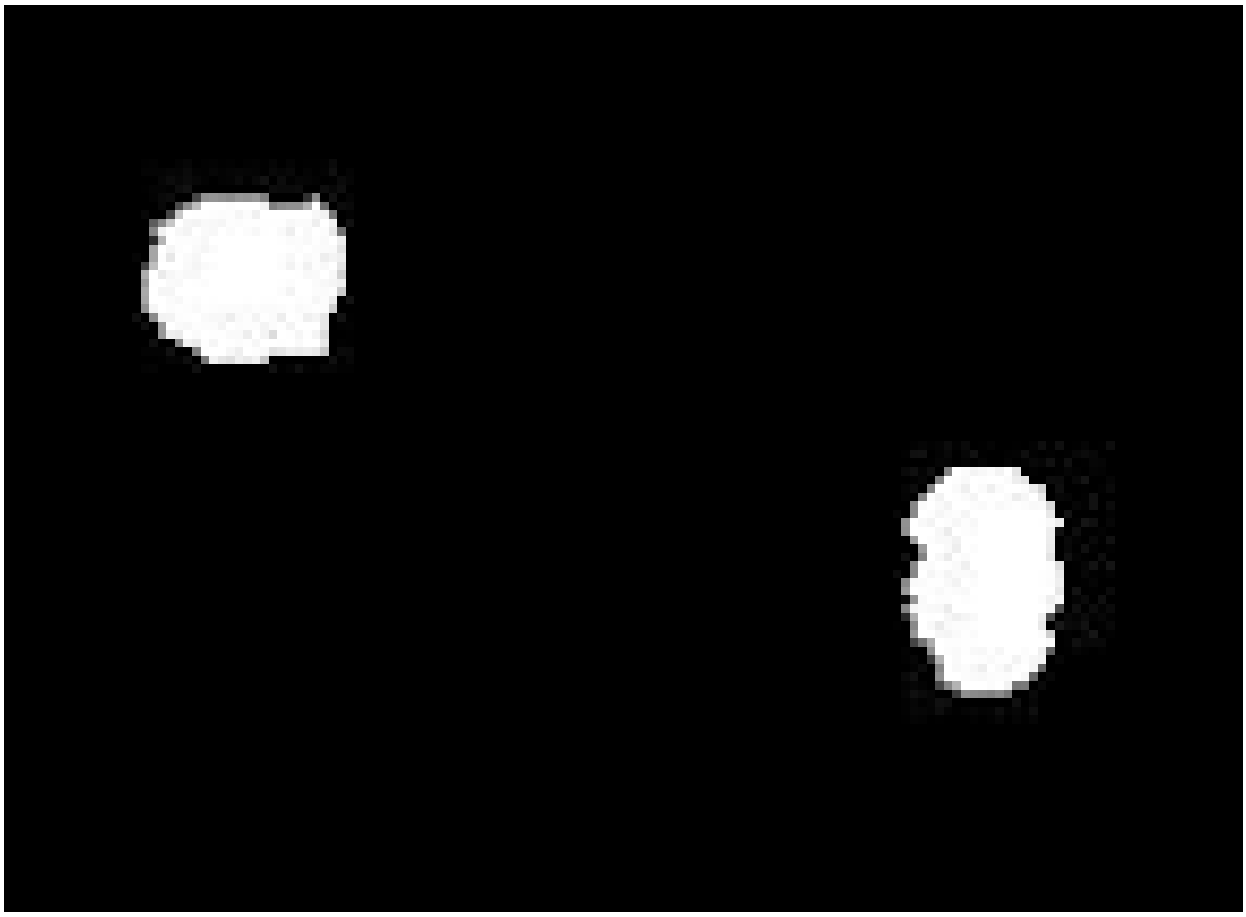

Figure 4: Representation of Otsu's method of binarization on a single image slice.

To binarize the image stack, a thresholding value—referred to as sensitivity—was required, and ranges from zero to one. To get a quick idea of thresholding value's impact, 3D image stacks were maximum projected along the z-axis to produce 2D images, enabling faster processing and

then binarized. The following four sensitivity values were tested: 0.01, 0.1, 0.25, and 0.35. The resulting binary stacks were compared to the original image stacks to see which one best highlights the cellular regions. (See Section 3.1 for results and Section 4.1 for discussion.)

2.2.2 Morphological Analysis

The tool is developed to conduct 2D and 3D analyses. Using the binarized 3D stack, the code extracts the volumes, centroids, eigenvectors, and eigenvalues of the cellular structures. from ImageJ (x: 1.1347 µm/pixel, y: 1.1347 µm/pixel, z: 10 µm/slice). With the 2D max-projected binarized image, the circularity, orientation, major axis lengths, and minor axis lengths of the cellular structures are extracted.

Circularity: this property quantifies the roundness of a cell using Eq. 1. The maximum value is one. Higher roundness of the cell will be indicated by a higher value.

$$Circularity = \left(\frac{4\pi * area}{perimeter^2}\right) \quad (1)$$

Orientation: The elongated cell is fit to an ellipse and this property reports the angle between the x-axis and the ellipse's axis.

Major and Minor Axis Lengths: returns the length of the major and minor axes, in pixels, of an ellipse. Here, the function fits the elongated cells to an ellipse.

2.3 Cell Orientation Analysis

2.3.1 Determining Nearest Neighboring Cells and Distance

The code used a distance-based thresholding approach to identify a cell's nearest neighbor. Based on preliminary calculations, an initial threshold of 375 microns was determined. With this as a basis, the code calculated distances between cell centroids. If the distance between pair of cells was found to be at the same as the threshold value, that pair of cells is saved. Furthermore, if

the distance is closer than the current threshold, the threshold is updated to the smaller distance. This process was repeated for all cell pairs, and the resulting distances were stored in a vector.

2.3.2 Angles Between Neighboring Cells and the Dot Product

The vector in the x and y directions for the cells were computed by taking the cosine and sine of the angle resulting from the orientation output. Then, the dot product was taken between the vectors to determine the degree of alignment between pairs of neighboring cells. The dot product is from zero to one, and a higher value indicated more alignment between the cells. Likewise, taking the inverse cosine of the dot product yielded the angle between the pairs of neighboring cells.

2.3.3 Plots

Using the data obtained in 2.3.1 and 2.3.2, a dot product versus distance scatter plot and a circularity versus distance scatter plot were created.

2.4 Statistical Analysis

2.4.1 Test for Normality

Prior to any statistical analysis, the dot products and circularity of the cells were tested for normality using Quantile-Quantile (QQ) plots. If the data was found to follow a normal distribution, an Anova test was conducted on subsequent statistical analysis, while a Kruskal Wallis test was used for data that did not follow a normal distribution.

2.4.2 Distance Groupings and Statistics

Before the Anova or Kruskal Wallis test, the dot product and circularity data are grouped based on the distance between neighboring cells, as described in 2.3.1. Group 1 consists of distances between 0-88 microns, group 2 is 88-117 microns, group 3 is 117-148 microns, group 4

is 148-174 microns, and group 5 is anything greater than 184 microns. These groupings were chosen to ensure that each set has a similar sample size.

2.4.3 One Sample Kolmogorov Smirnov Test

A one sample Kolmogorov Smirnov (KS) test was conducted to check if the data came from a standard normal distribution, determined at a 5% significance, alongside the respective p-value. This test is performed on the angles and dot products between the neighboring cells.

2.4.4 Two Sample Kolmogorov Smirnov Test

Likewise, a two-sample KS test was performed to see if the two samples come from the same continuous distribution. For the dot products and circularities, group one (0-88 microns) was compared with every other group. The test was performed at a 5% significance. In addition, the empirical continuous distribution plots were made for data in group one and that of group five.

2.4.5 Histogram Plots

The angles between the pairs of cells were plotted on a polar histogram to get insight on its distribution. As the variance of distance is an important factor in this study, angles that stem from group one and that of group five are overlayed on the plot.

CHAPTER 3: RESULTS

3.1 Sensitivity Analysis Results

The results in this section are a representative case of a single position in gel one. This analysis is carried out for all positions in each gel. Data presented in 3.2 onwards represent the aggregate of the gels produced in triplicate.

Figures 5A-5E show the impact of varying sensitivities on the 2D image projection of a single position in a gel.

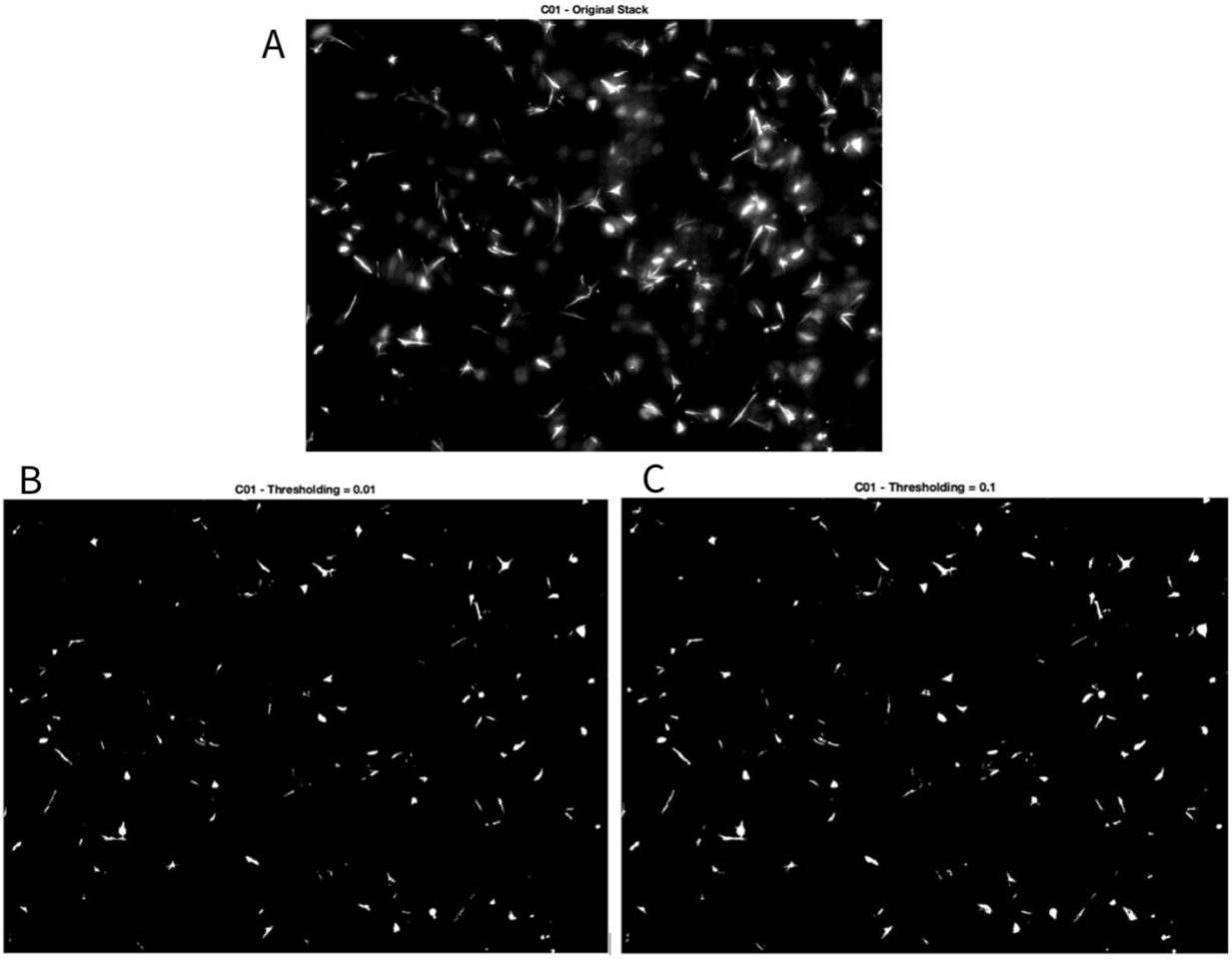

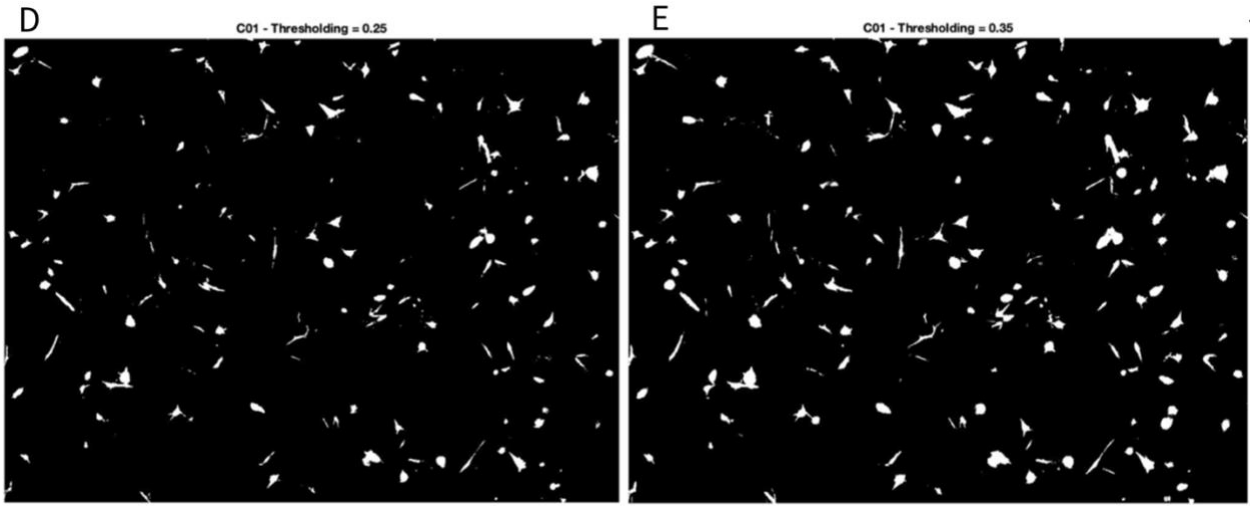

Figure 5: Impact of varying sensitivities on the 2D images. (A) original 2D C01 image. (B) Thresholding of 0.01. (C) Thresholding of 0.1. (D) Thresholding of 0.25. (E) Thresholding of 0.35.

3.2 Test for Normality

The aggregate circularity and dot products were plotted on a QQ-plot to determine if they follow a normal distribution. From figures 6A and 6B, it is evident that the data does not follow the standard red line, meaning that neither dataset follow a normal distribution. Therefore, Kruskal Wallis tests were performed to determine statistical significance on the dot products and circularities with distance.

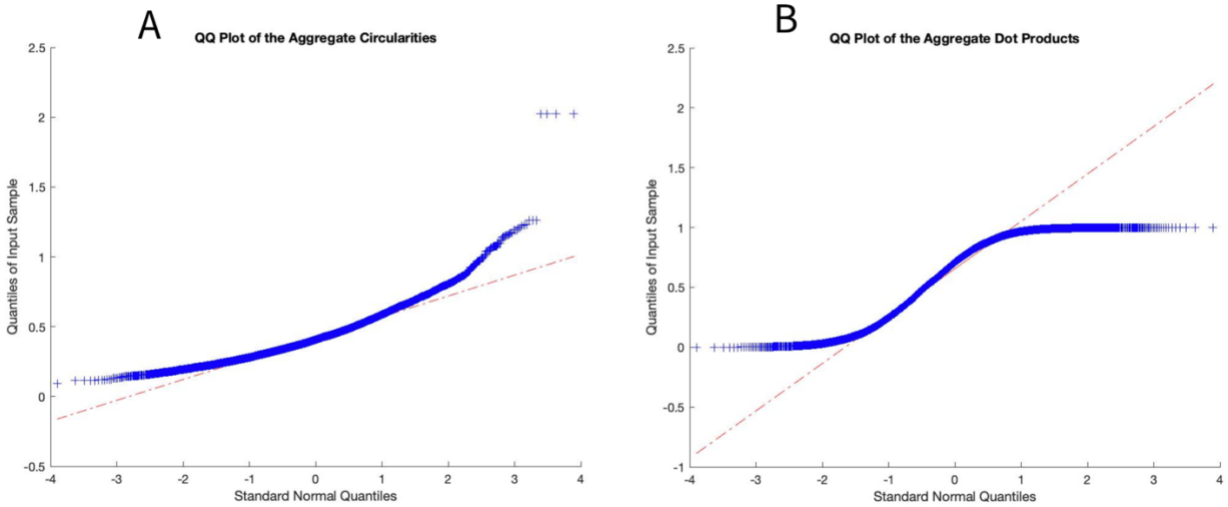

Figure 6: QQ plots showcasing normality of the data. (A) QQ plot showcasing the aggregate circularities. (B) QQ plot showcasing the aggregate dot products.

3.3 Kruskal Wallis Tests

As the distribution of average circularities and dot products were not normal, Kruskal Wallis tests were performed to gain insight on how varying the distance between pairs of neighboring cells has an impact on cell elongation (circularities) and alignment (dot products).

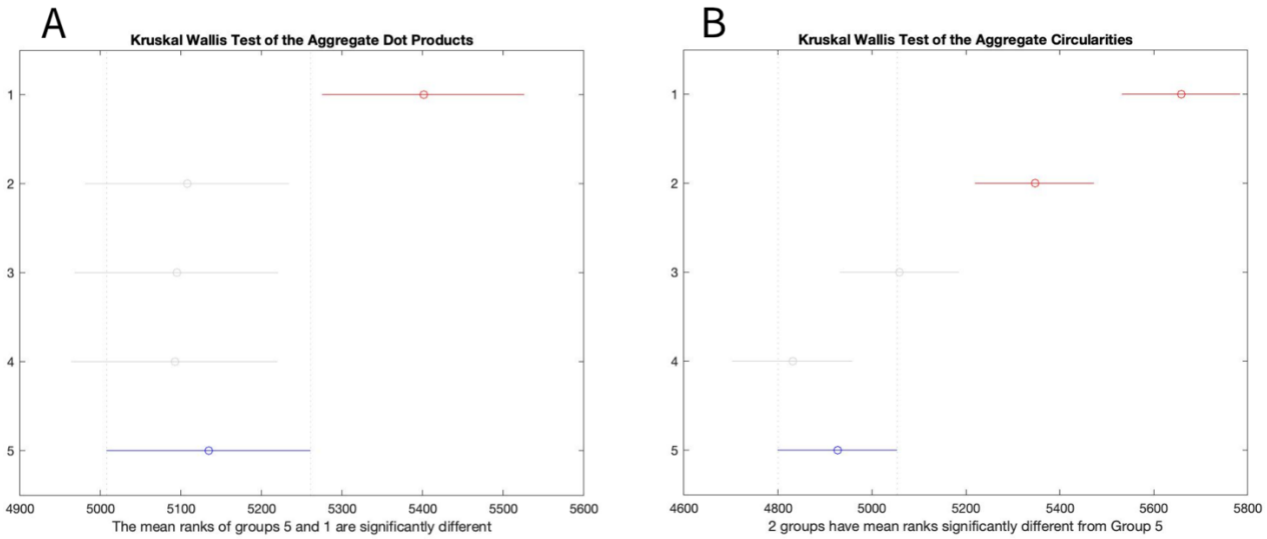

Figure 7: Multi-stat plot from the Kruskal Wallis Test. (A) Kruskal Wallis plot of dot products comparing the means ranks of each distancing group. (B) Kruskal Wallis plot of circularities comparing the means ranks of each distancing group.

Table 1: Aggregate Kruskal Wallis Test Results for the Circularities.

Group	Results
1	Groups 2, 3, 4, and 5 have statistically significant mean ranks from Group 1
2	Groups 1, 3, 4 and 5 have statistically significant mean ranks from Group 2
3	Groups 1 and 2 have statistically significant mean ranks from Group 3
4	Groups 1 and 2 have statistically significant mean ranks from Group 4
5	Groups 1 and 2 have statistically significant mean ranks from Group 5

The Kruskal Wallis test on the circularities are summarized in table 1. A larger mean rank indicates that the values in that group tend to be higher, while a lower mean rank indicates that values in that group tend to be smaller. Group 1 has the highest mean rank of 5,689 and is

statistically significant from the rest of the groups. Group 2 has the second highest mean rank of 5,347 and is also statistically significant from the remaining groups. Group 3 has a mean rank of 5,059 and is statistically significant from groups 1 and 2. Likewise, groups 4 and 5 and have mean ranks of 4,381 and 4,927, respectively, and both are statistically significant from groups 1 and 2. These tests were performed with a resulting p-value of 0.

Table 2: Aggregate Kruskal Wallis Test Results for the Dot Products

Group	Results
1	Groups 2, 3, 4, and 5 have statistically significant mean ranks from Group 1
2	Group 1 has a statistically significant mean rank than Group 2
3	Group 1 has a statistically significant mean rank than Group 3
4	Group 1 has a statistically significant mean rank than Group 4
5	Group 1 has a statistically significant mean rank than Group 5

Similarly, the Kruskal Wallis test was performed on the dot products and summarized in table 2. Group 1 has a mean rank of 5,401 and is statistically significant from the rest of the groups. Group 2 has a mean rank of 5,108 and is also statistically significant from group 1. Like group 2, groups 3-5 are only statistically different from group 1, with mean ranks of 5,095, 5,092, and 5,134, respectively. These tests were performed with a resulting p-value of 0.0024.

Alongside the Kruskal Wallis tests, the respective box plots were given as well in fig 8A and 8B, in which the y-axis represents the value of interest (circularity or dot products).

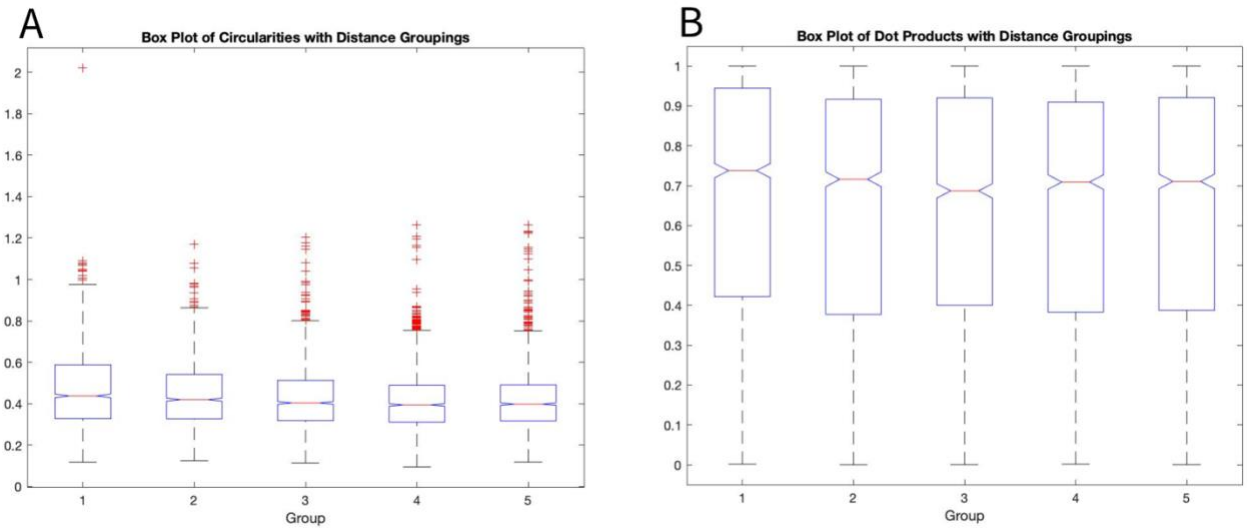

Figure 8: Box plots of the circularities and dot products. (A) Box plot of the aggregate circularity data against distance groups. (B) Box plot of the aggregate dot products against distance groups.

To gain further insight of the data's distribution, the mean, median, and standard deviations of circularities and dot products of each distance group were computed and summarized in the tables 3 and 4, respectively. Also, the number of samples in each group of distance is presented as well.

Table 3: Means, medians, standard deviations (stdv), and sample size of the aggregate circularity data based on distance groupings.

Distance Group	Mean ± Stdv	Median	# Samples
1	0.4667 ± 0.1911	0.4378	2,105
2	0.4418 ± 0.1568	0.4198	2,055
3	0.4269 ± 0.1530	0.4038	2,074
4	0.4144 ± 0.1473	0.3942	2,033
5	0.4196 ± 0.1484	0.3981	2,066

Table 4: Means, standard deviations, and sample size of the aggregate dot products based on distance groupings.

Distance Group	Mean ± Stdv	Median	# Samples
1	0.6592 ± 0.3075	0.7377	2,105
2	0.6324 ± 0.3108	0.7161	2,055
3	0.6316 ± 0.3052	0.6870	2,074
4	0.6329 ± 0.3063	0.7091	2,033
5	0.6356 ± 0.3080	0.7107	2,066

3.4 One-Sample and Two-Sample Kolmogorov-Smirnov Tests

One-sample Kolmogorov Smirnov tests were applied on the distribution of angles (both aggregate and by distance groups). The null hypothesis was that the distribution does follow a uniform distribution, while the alternate says it does not. A uniform distribution indicates that cells do not preferentially align, while a non-uniform distribution indicates preferential alignment. Results in table 5 said that the aggregate distribution of the angles between cells may follow a uniform distribution. However, when splitting it by distance groups, it is found that angles in group 1 of distances (0-88 microns) may not follow a uniform distribution while the remaining groups do, presented in table 6. So, cells may exhibit preferential alignment when they are closer apart, while that may not happen as cells are farther apart.

Likewise, the one-sample Kolmogorov Smirnov test was done on the dot products by distance groupings, presented in table 7. The results indicate that the dot products do not come from a uniform distribution in any distance group, meaning cells may exhibit some degree of preferential alignment even at increasing distances.

Table 5: One-Sample KS test results of the aggregate data of angles between cells compared against a uniform distribution of angles.

Metric	Results for Angle Distribution
Rejecting null Hypothesis?	No
p-value	0.1316

Table 6: One-Sample KS test results of the angles between cells compared against a uniform distribution of angles based on distance groupings.

Group	Reject Null Hypothesis?	p-value
1	Yes	4.0322×10^{-4}
2	No	0.3854
3	No	0.1240
4	No	0.0627
5	No	0.7043

Table 7: One-Sample KS test results of the dot products between cells compared against a uniform distribution of angles based on distance groupings.

Group	Reject Null Hypothesis?	p-value
1	Yes	4.5916×10^{-115}
2	Yes	6.8091×10^{-86}
3	Yes	7.4024×10^{-77}
4	Yes	1.3634×10^{-79}
5	Yes	4.8838×10^{-88}

A two-sample Kolmogorov Smirnov test was performed on the dot products and average circularities based on distance groupings. Data in group 1 was compared with every other group to see if both groups may follow the same continuous distribution (the null hypothesis). If they do follow the same distribution, it indicates that varying distance might not influence cell alignment and elongation. If the groups do not follow the same distribution (the alternate hypothesis), then it indicates that varying distance does influence cell elongation and alignment.

For the dot products, when group 1 was compared with groups 2-5, it was found that none of them follow the same continuous distribution. This could mean that cells closer together may exhibit different behavior for alignment closer together than farther apart.

For the average circularities, a similar result was found where groups 2-5 do not follow the same continuous distribution as group 1. This indicates that cell elongation is different for cells closer together compared to farther apart.

Table 8: Two-Sample KS test results for the dot products based on distance groupings.

Group	Reject Null Hypothesis?	p-value
1 vs 2	Yes	0.0085
1 vs 3	Yes	9.5334×10^{-4}
1 vs 4	Yes	7.8189×10^{-4}
1 vs 5	Yes	0.0129

Table 9: Two-Sample KS test results for the aggregate circularities based on distance groupings.

Group	Reject Null Hypothesis?	p-value
1 vs 2	Yes	1.4019×10^{-6}
1 vs 3	Yes	2.0188×10^{-13}
1 vs 4	Yes	4.0307×10^{-22}

1 vs 5	Yes	4.8369×10^{-21}

Alongside the two-sample Kolmogorov Smirnov tests, empirical cumulative distribution (ecdf) plots of the dot products, circularities, and angles comparing groups 1 and 5 are given below. These plots provide insight on how the data is distributed and if they change for varied distances between cells. The x-axis represents the dot products.

For the dot products, the graph gradually increases, showcasing that the data is more spread out. Towards the 0.9-1 range, there is a steep slope, indicating that the data is clustering in that area. As the trend of the plots look similar for groups 1 and 5, it can indicate that the distribution of dot products is similar even at varied distances between cells.

For the average circularities, a sharp peak is observed around the 0.3-0.45 range for both plots and plateaus at 1. However, the curve is steeper for group 5 than group 1. This shows that majority of the average circularity data is clustered in the 0.3-0.45 range for both groups, in which the data in group 5 is clustered a lot more in that region than group 1.

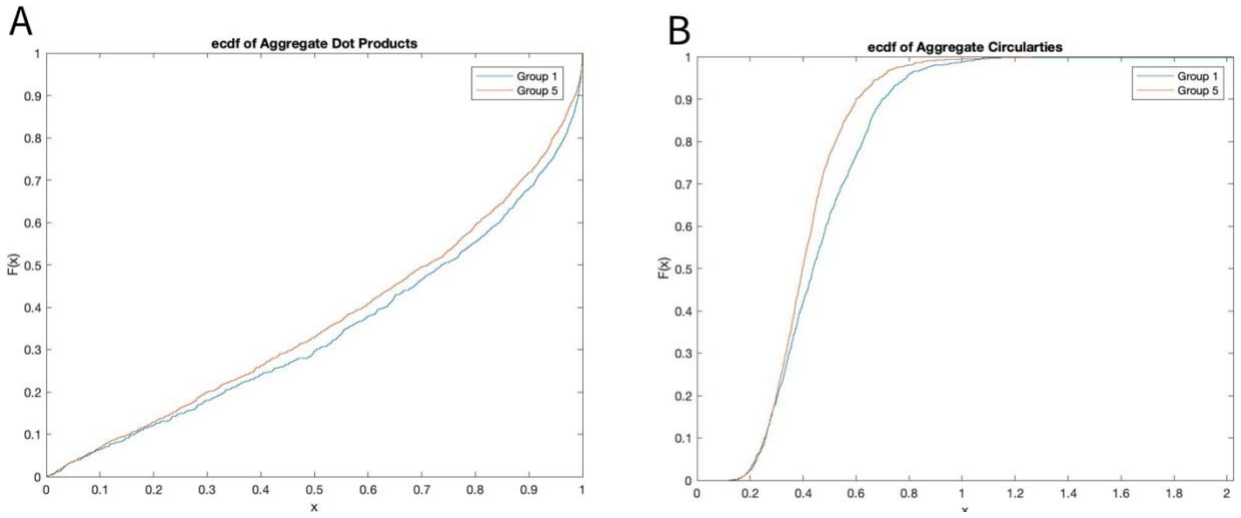

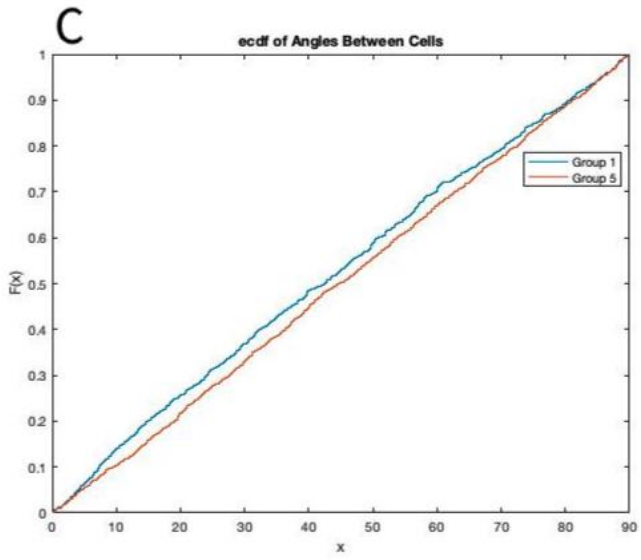

Figure 9: Empirical cumulative distribution function (ecdf) plots. (A) ecdf plot of the aggregate dot products. (B) ecdf plot of the aggregate circularities. (C) ecdf plot of the angles between cells.

3.5 Polar Histogram

The angles between cells are plotted on a polar histogram plot to see the distribution of the data. The aggregate angles are plotted as well as angles in group 1 and 5. Smaller angles indicate more alignment between cells, while larger angles indicate the opposite.

Figure 10A shows the distribution of angles in group 1 of distances against the angles in group 5. There is more favoring towards smaller angles for group 1, particularly in the 0-30 degrees range. However, for group 5, angles seem to favor less of the smaller angles, peaking in 45–60-degree range. So, it is possible that cells closer to each other do experience alignment with one another compared to cells farther apart, therefore showcasing preferential alignment

Figure 10B shows the distribution of the aggregate angles. It appears more uniform compared to figure 10A. So, on the large scale, the distributions of angles may appear to not showcase preferential alignment. However, when breaking into the specific groups, it is evident that the cells do showcase some degree of preferential alignment closer together than farther apart.

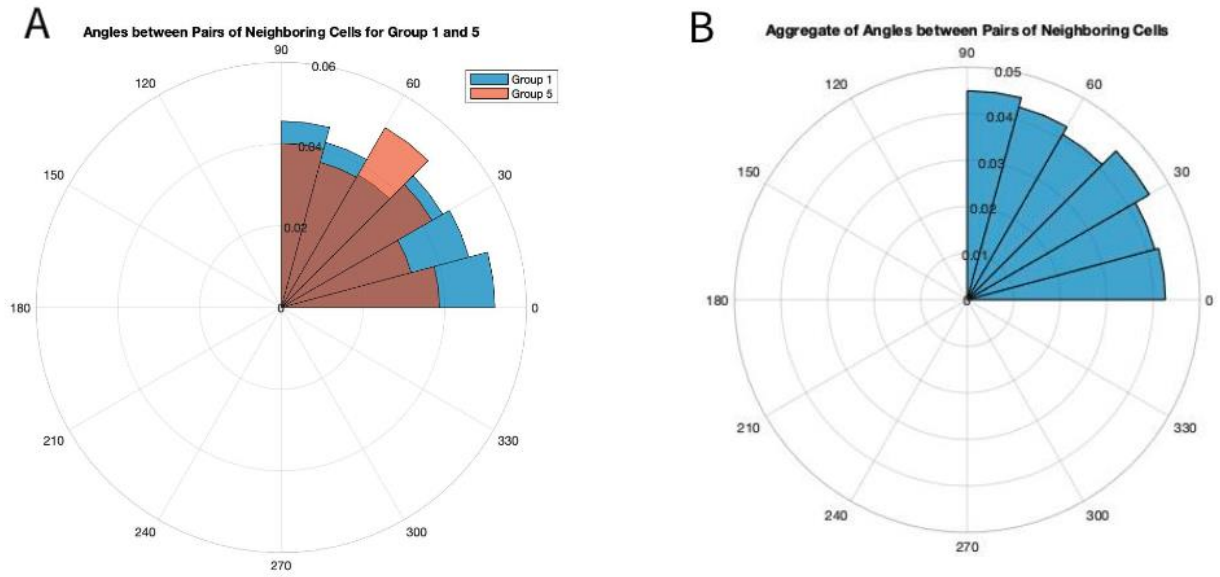

Figure 10: Polar histogram plot of the angles between cells. (A) Polar histogram of the angles between pairs of neighboring cells for distance group one vs five. (B) Polar histogram of the aggregate of angles.

3.6 Scatter Plots

Finally, a scatter plot of the dot products and average circularities were plotted against distance to get insight on how the data is spread and see if any correlations can be made with varying distances.

For the dot products, it is unclear as to dot products relate with varying distances due to the vast spread of the data. Likewise, the spread of average circularities is high, yielding a similar conclusion. Furthermore, a correlation coefficient was computed to get further quantitative insight on distance versus dot products and circularities. For distance and dot products, the coefficient is -0.0192 with a p-value of 0.056, and the coefficient for distance versus circularities is -0.1004 with a p-value of 0.

Both datasets have a weakly negative linear relationship, meaning as distance increases, the dot products and circularities tend to decrease. This indicates that there may be more alignment and less elongation when cells are closer together while cells tend to be less aligned and more

elongated at farther distances. The results of the circularities are not as initially expected, while the results for the dot products are following initial expectations.

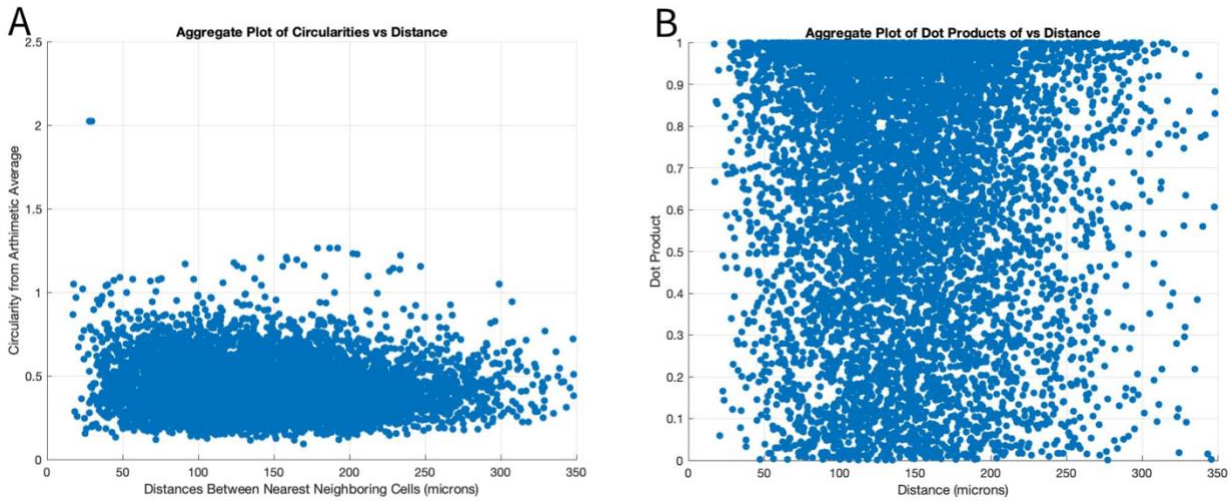

Figure 11: Scatter plots of circularities and dot products against varying distances. (A) Scatter plot of the aggregate circularities. (B) Scatter plot of the aggregate dot products.

CHAPTER 4: DISCUSSION

4.1 Sensitivity Analysis Results

The purpose of the sensitivity testing was to determine a proper thresholding value and refine the image to focus better on the cellular regions. Figures 5A-5E shows the original max projected C01 image stack and the binarization results with varying sensitivity values. In figure 12, the brighter regions were found to be the cells of interest; these were the cells closer to the imaging scope. However, the cells closer to the bottom of the gel appeared as smears. A closer look of figure 5 is provided in figure 12 where the red region is represents the cells closer to the bottom of the gel and the blue regions are the cells closer to the top. The cells at the bottom of the gel are not of interest as they may be influenced due to their adhesion to the glass.

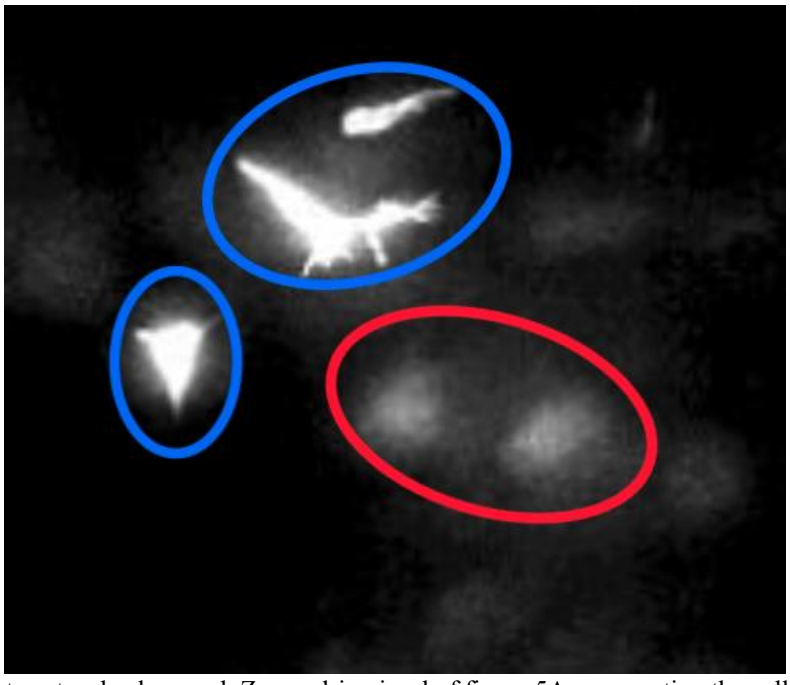

Figure 12: Cells of interest vs background. Zoomed-in visual of figure 5A representing the cells closer to the scope (blue) and farther away from the scope (red).

Figures 13A-13E represents a zoomed-in region of figures 5A-5E and showcases the results of each binarization. Sensitivity levels of 0.01 and 0.1 were determined to be too stringent

as the cellular structures were not fully preserved, showcased by 13B and 13C when compared to 13A. Sensitivities of 0.25, in fig 13D, better captures the cellular region, but it fails to capture the stretched ends. Ultimately, at 0.35, it captures all the cellular space. Therefore, a sensitivity of 0.35 was determined to be the appropriate thresholding level.

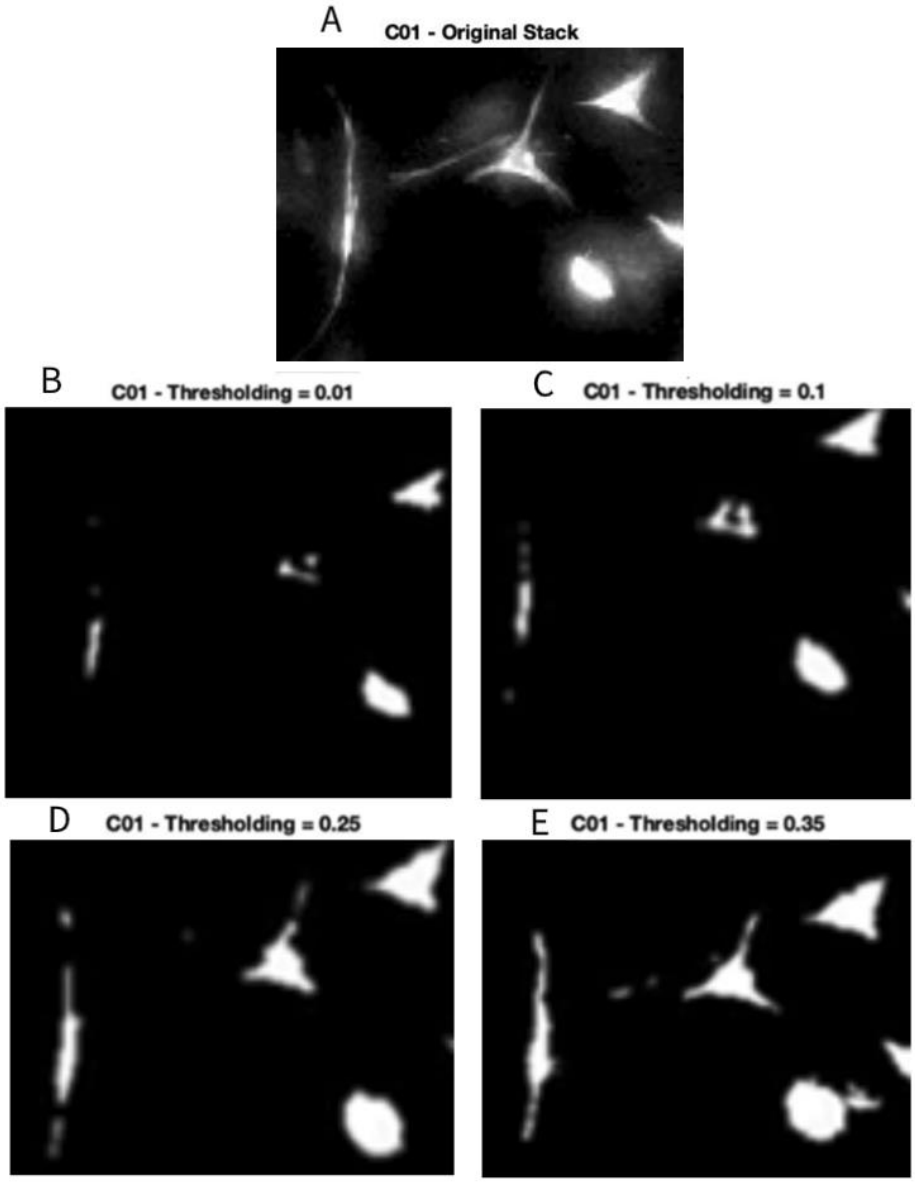

Figure 13: Zoomed-in regions of figures 5A-5E showcasing the result of varying binarization levels.

4.2 Analysis of Cell Elongation - Average Circularities

An aspect of this project was to see how cells elongate with one another as the distance between cells are varied. Based on existing literature and studies, cells should elongate more towards each other with closer proximity and elongate less as the distance is increased. In other words, the average circularity between pairs of cells should be lower as cells are closer and should increase with more distance.

The two-sample Kolmogorov Smirnov tests yielded that varying distance between cells does influence cell elongation as the average circularities in groups 2-5 do not follow the same continuous distribution as the average circularities in group 1.

However, when looking at figure 7B for the Kruskal Wallis test results, it showed that the average circularities in group 1 tend to be higher than the other groups due to group 1 having the highest mean rank. This is further supported by the values in table 1. This means that cells closer to each other are not elongating towards one another. As the distance between them is increased the circularity decreases, meaning the pairs of cells are elongating more. This finding is opposite of what was observed with contact guidance, where cells tend to elongate more when closer together.

There are a few possibilities for this. One could be due to the 24-hour incubation time used in this study. In the study performed by Thrivikraman *et al.*, after the final gel composition was made, an incubation time of 8 hours was used to allow the cells to spread, giving scope on contact guidance behavior.[3] However, in this study, the gels are incubated for 24 hours, meaning a lot more interactions are occurring. Specifically, the longer incubation time can give insight on if cells remodel themselves with the gel rather than just allowing the initial spreading. Redoing the gel formation with a shorter incubation time can might give better insight on how cells elongate and

migrate along the fibrin gel. Also, there is a possibility that the cells are not remodeling themselves enough with the gel, which could yield to cells not elongating towards one another when they are closer.

Another possibility could be due to the higher seeding density of cells into the fibrin gels. Again, the study in Thrivikraman *et al.* used a cell concentration of 20,000 cells/mL for each gel while this study used 30,000 cells/mL.[3] In the crowded environments, cells have less freedom to reorient and migrate, which can weaken the effects of contact guidance and rather emphasize the effects of cell-adhesion over cell-ECM signaling. Tying back to the discussion of cell remodeling, there could be enough remodeling happening to a point where the analysis would need to be redone as a network of cells rather than comparison between two cells. One way to verify and mitigate this is by calculating the distance between cells using the closest surfaces rather than the centroids. This will provide a better idea of how far apart cells are and give insight on impacts of higher cell seeding densities. The code can be changed to incorporate these needs, which can help provide better insight of cell contact guidance as a system.

Putting this together, the statistical analysis on the average circularities showcased that cells tend to elongate more towards one another when the cells are farther apart compared to being closer together, which does not match with initial expectations. Possibilities of why this trend is seen were discussed above, and alternative tests were discussed as well, giving scope for further investigation.

4.3 Analysis of Cell Alignment - Dot Products

The dot product was computed between pairs of neighboring cells to gain insight on how cells align with one another as the distance between them is varied. A higher dot product value indicates a higher degree of alignment between pairs of cells.

From the one-sample Kolmogorov Smirnov test, it was evident that cells may exhibit some degree of preferential alignment across all distances. This finding was strengthened by the results of the two-sample Kolmogorov Smirnov tests as the distribution of dot products do not follow the same continuous distribution as the dot products in groups 2-5. For the closer distances, these results match the expectations as cells tend to align with one another via contact guidance. There was some degree of preferential alignment even at farther distances, giving insight that contact guidance behaviors could potentially be present at farther distances, though at weaker levels. However, when the dot product distributions of groups 2-5 were compared against each other using the two-sample Kolmogorov Smirnov tests, it was noted that they may come from the same continuous distribution, indicating that varying distance from 117 and higher does not influence cell alignment. This is further supported by the Kruskal Wallis tests as only group 1 had the highest statistically significant mean rank, and the others were not statistically significant of each other.

Furthermore, when these findings were tied to the findings of the average circularities, the data said that cells tend not to elongate towards one another when closer together but have a higher degree of alignment. As the distance between cells are increased, cells tend to elongate more while aligning less. Though the cell alignment behavior of cells may follow expectations, it faltered when tied with the average circularities.

One reason for this trend could be due to orientation of cells when they align and how the dot product is calculated. In the current version of the code, it cannot distinguish the types of alignment shown in figures 14A and 14B. Per the dot product calculation, both configurations have the same dot product even though they are both separated by the same distance (denoted x in the figure). However, the forces acting upon the cells to be in those orientations may be different and cannot be captured and distinguished with the code.

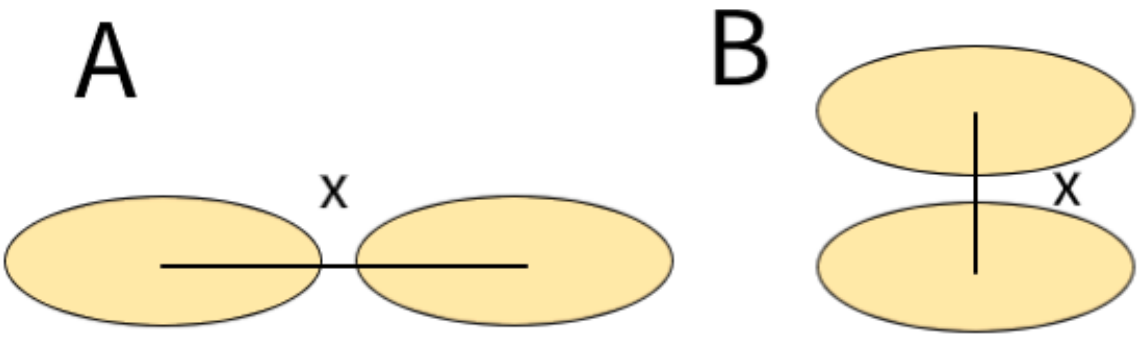

Figure 14: Types of cell orientation while maintaining same distance.

One way to mitigate this is to modify the calculation of the distance between cells by adding a directionality component. Instead of just using the centroids of the cells, incorporating the orientation vector or eigenvectors of the cells can incorporate directionality of the cells. With this incorporation, the dot products will be different for both configuration of cell alignment shown in figures 14A and 14B. The code can obtain the eigenvectors of the cells, making this adjustment feasible.

In summary, cells showcase behaviors of higher alignment with one another as they are closer and less alignment as the cells are farther apart. There is improvement opportunities present in dot product calculations, discussed above, that can give better insight regarding cell alignment in future applications of this code.

4.4 Analysis of Cell Alignment - Angles Formed Between Cells

Finally, cell alignment was also assessed by analyzing the angles between the pairs of cells. A smaller angle indicates more alignment between cells. Like the findings for the dot products, cells experience more alignment with one another closer together than farther apart, as shown in the polar histogram plot. This follows the expectations laid out in the literatures and similar studies.

The one-sample Kolmogorov Smirnov tests for each distance groups reveals that cells only between 0-88 microns apart tend to exhibit preferential alignment, while the remaining groups do

not. This behavior seems to align with the initial expectations but is different when tied together with the findings on cell elongation.

As discussed in section 4.2, there could be a possibility that cells are touching each other, which triggers cell adhesion rather than cell-ECM signaling. Fibroblasts can participate in cadherin-based binding when they touch, which is different from proteins in cell-ECM signaling. As mentioned in sections 4.2 and 4.3, altering the distance calculation to be based on the closest surfaces of the cells and incorporating a directionality component, such as the eigenvector, can provide a better idea of how the variation of distance between cells influences their ability to align with one another.

4.5 Summary of Results

Overall, the statistical tests give us insight on how distance between cells affects the elongation and cell alignment. The dot product and angle between cells showcased trends of cells having more alignment when they are closer to one another, while the opposite trend was observed for the circularities. With the findings, no conclusions can be made from the data and statistical tests due to these contradicting trends, meaning there are opportunities for improvements in the computational tool, which are discussed in chapter 5.

CHAPTER 5: SUMMARY, IMPROVEMENTS, & FUTURE SCOPE

5.1 Summary

The goal of this study is to develop a foundational computational tool that can help quantify the observed effects of cell contact guidance. Cells were cultured and curated into fibrin gels and stained to separately see the cell's cytoskeletal and structures and nucleus. After the gels were imaged via microscopy, the image-stacks were uploaded into the computational tool to analyze cell elongation, via the circularity factor and alignment, via the dot products and angles formed between cells, against varying distance. It was expected that cells closer to one another will be more aligned and elongated, meaning the dot product is higher and circularity is lower. As the distance increases, the dot product should decrease while circularity should increase.

The dot products were higher when cells are closer together, indicating more alignment with one another. However, the average circularities showed the opposite trend, where it was higher for cells closer together and decreased as cells went farther apart. Due to these contradicted trends, alongside the results from the statistical analyses, no strong conclusions can be drawn.

5.2 Improvement Opportunities

5.2.1 Circularity Calculation

Formula 1 shows the equation used to calculate circularity in this study. However, when analyzing the data for average circularities, there were a few instances where the average circularity value exceeded one. Upon investigation, it was noted that MATLAB updated their formula to calculate circularity with Eq. 2.

$$Circularity = \left(\frac{4\pi * area}{perimeter^2}\right) * \left(1 - \frac{0.5}{r}\right)^2, where\ r = \frac{perimeter}{2\pi} + 0.5 \quad (2)$$

This was found towards the end of the study, so the change could not be incorporated. In the future, running the most up to date version of MATLAB will ensure the proper formulas are used. However, for the purpose of this study, this discrepancy did not cause issues as the number of data points that exceeded one made up ~0.6% of the dataset. Per MATLAB updates, Eq. 1 had bias of calculating too high of a circularity for relatively small objects. This factor could have been why the average circularities had erroneous values.

5.3 Future Scope

To further develop this tool and understand the data, the tests can be redone with a lower cell seeding density, like what was done in Trivikraman et al. With a lower cell concentration in the fibrin gels, contact guidance may be more pronounced and provide better insight of the data.

Furthermore, the analyses performed in this study can be extended into the 3D space. Instead of circularity, the cellular regions can be characterized by a volumetric factor defined as the volume of the cell divided by the volume of the cellular region fit to the nearest ellipsoid. This can help eliminate the issue mentioned in section 5.2 regarding overlap of cellular regions when max projected into 2D.

Another aspect to explore is using collagen gels instead of fibrin gels. Collagens are the most abundant proteins present in the ECM that play a crucial role in structural support and signaling.[15] Understanding how cells signal and migrate in collagen gels can also provide useful insight of cell behavior, which can be then extended to diseases states and development of therapeutics.

BIBLIOGRAPHY

1. Seigel, R., Giaquinto, A., Jemal, A. Cancer Statistics, 2024. American Cancer Society.
2. Walker, C., Mojares, E., Hernandez, A. Role of Extracellular Matrix in Development and Cancer Progression. *International Journal of Molecular Sciences.*
3. Thrivikraman, G. *et al*. Cell contact guidance via sensing anisotropy of network mechanical resistance. Proc. Natl. Acad. Sci. U. S. A. 118, e2024942118 (2021).
4. Estabridis, H. M., Jana, A., Nain, A. & Odde, D. J. Cell Migration in 1D and 2D Nanofiber Microenvironments. *Ann. Biomed. Eng.* **46**, 392-403 (2018).
5. Ray, A. *et al*. Anisotropic forces from spatially constrained focal adhesions mediate contact guidance directed cell migration. *Nat. Commun*. **8**, 14923 (2017).
6. Dickinson, R. B., Guido, S. & Tranquillo, R. T. Biased cell migration of fibroblasts exhibiting contact guidance on well-defined micro- and nanostructured substrates. *Ann. Biomed. Eng.* **22**, 342-356 (1994).
7. Tamiello, C. *et al*. Heading in the Right Direction: Understanding Cellular Orientation Responses to Complex Biophysical Environments. *Biomedical Engineering Society.*
8. Bangasser, B. L. & Odde, D. J. Master equation-based analysis of a motor-clutch model for cell traction force. *Cell. Mol. Bioeng.* **6**, 449–459 (2013).
9. Feng, J., Levine, H., Mao, X. & Sander, L. M. Cell motility, contact guidance, and durotaxis. *Soft Matter* **15**, 4856– 4864 (2019).
10. Prahl, L. S., Stanslaski, M. R., Vargas, P., Piel, M. & Odde, D. J. Predicting Confined 1D Cell Migration from Parameters Calibrated to a 2D Motor-Clutch Model. *Biophys. J.* **118**, 1709–1720 (2020).
11. Dorsey, T. B. *et al.* Evaluation of photochemistry reaction kinetics to pattern bioactive proteins on hydrogels for biological applications. *Bioact. Mater.* **3**, 64–73 (2017).
12. Hong, H. *et al*. Grayscale mask-assisted photochemical crosslinking for a dense collagen construct with stiffness gradient. *J. Biomed. Mater. Res. B Appl. Biomater.* **108**, 1000–1009 (2020).
13. Sunyer, R., Jin, A. J., Nossal, R. & Sackett, D. L. Fabrication of Hydrogels with Steep Stiffness Gradients for Studying Cell Mechanical Response. *PLOS ONE* **7**, e46107 (2012).
14. Otsu, N. A Threshold Selection Method from Gray-Level Histograms." *IEEE Transactions on Systems, Man, and Cybernetics.* Vol. 9, No. 1, 1979, pp. 62-66.
15. Shakiba, D. *et al*. The Balance between Actomyosin Contractility and Microtubule Polymerization Regulates Hierarchical Protrusions That Govern Efficient Fibroblast-Collagen Interactions. *National Library of Medicine.*